frontiers in Marine Science

ORIGINAL RESEARCH
published: 27 November 2018
doi: 10.3389/fmars.2018.00446

Regionalization and Dynamic Parameterization of Quantum Yield of Photosynthesis to Improve the Ocean Primary Production Estimates From Remote Sensing

Maria Laura Zoffoli[1*†], *Zhongping Lee*[1] *and John F. Marra*[2]

[1] School of the Environment, University of Massachusetts, Boston, MA, United States, [2] Department of Earth and Environmental Sciences, Brooklyn College (CUNY), Brooklyn, NY, United States

Quantum yield of photosynthesis (ϕ) expresses the efficiency of phytoplankton carbon fixation given certain amount of absorbed light. This photophysiological parameter is key to obtaining reliable estimates of primary production (PP_{sat}) in the ocean based on remote sensing information. Several works have shown that ϕ changes temporally, vertically, and horizontally in the ocean. One of the primary factors ruling its variability is light intensity and thereby, it can be modeled as a function of Photosynthetically Available Radiation (PAR). We estimated ϕ utilizing long time-series collected in the North Subtropical Oligotrophic Gyres, at HOT and BATS stations (Pacific and Atlantic oceans, respectively). Subsequently the maximum quantum yield (ϕ_m) and K_ϕ (PAR value at half ϕ_m) were calculated. Median ϕ_m values were ~0.040 and 0.063 mol C mol photons^{-1} at HOT and BATS, respectively, with higher values in winter. K_ϕ values were ~8.0 and 10.8 mol photons m^{-2} d^{-1} for HOT and BATS, respectively. Seasonal variability in K_ϕ showed its peak in summer. Dynamical parameterizations for both regions are indicated by their temporal behaviors, where ϕ_m is related to temperature at BATS while K_ϕ to PAR, in both stations. At HOT, ϕ_m was weakly related to temperature and its median annual value was used for the whole data series. Differences in the study areas, even though both belong to Subtropical Gyres, reinforced the demand for regional parameterizations in PP_{sat} models. Such parameterizations were finally included in a PP_{sat} model based on phytoplankton absorption ($PP_{sat-aphy-based}$), where results showed that the $PP_{sat-aphy-based}$ model coupled with dynamical parameterization improved PP_{sat} estimates. Compared with PP_{sat} estimates from the widely used VGPM, a model based on chlorophyll concentration ($PP_{sat-chl-based}$), $PP_{sat-aphy-based}$ reduced model-measurement differences from ~62.8 to ~8.3% at HOT, along with well-matched seasonal cycle of PP (R^2 = 0.76). There is not significant reduction in model-measurement differences between $PP_{sat-chl-based}$ and $PP_{sat-aphy-based}$ PP at BATS though (37.8 vs. 36.4%), but much

OPEN ACCESS

Edited by:
Astrid Bracher, Alfred Wegener Institut Helmholtz Zentrum für Polar und Meeresforschung, Germany

Reviewed by:
Toru Hirawake, Hokkaido University, Japan
Thomas Jackson, Plymouth Marine Laboratory, United Kingdom

***Correspondence:**
Maria Laura Zoffoli
laura.zoffoli@umb.edu

†Present Address:
Maria Laura Zoffoli, Remote Sensing & Benthic Ecology (RSBE), Faculté des Sciences et des Techniques, Université de Nantes, Nantes, France

Specialty section:
This article was submitted to Ocean Observation, a section of the journal Frontiers in Marine Science

Received: *14 March 2018*
Accepted: *06 November 2018*
Published: *27 November 2018*

Citation:
Zoffoli ML, Lee Z and Marra JF (2018) Regionalization and Dynamic Parameterization of Quantum Yield of Photosynthesis to Improve the Ocean Primary Production Estimates From Remote Sensing. Front. Mar. Sci. 5:446. doi: 10.3389/fmars.2018.00446

better agreement in seasonal cycles with $PP_{sat-aphy-based}$ (R^2 increased from 0.34 to 0.71). Our results point to improved estimation of PP_{sat} by parameterized quantum yield along with phytoplankton absorption coefficient at the core.

Keywords: ocean color, quantum yield of photosynthesis, phytoplankton primary production, marine seasonal variability, *in situ* measurements, dynamical parameterization

INTRODUCTION

Comprising a vast and highly dynamic area, the oceans are considered responsible for approximately half of global primary production (Field et al., 1998; Behrenfeld et al., 2001). Ocean color remote sensing provides multiple environmental parameters on a daily basis for the world oceans that have been widely used to model marine primary production (PP). However, no algorithms have shown a high performance in every oceanic region to retrieve PP based on satellite measurements. There are significant differences in estimated primary production from these models, which, broadly speaking, are based either on biological or optical information. Instead, regional adjustments of those algorithms seem to be key to obtain more accurate results, for example, based on marine biogeochemical provinces (Platt et al., 1991). Field campaigns are still needed for such regional calibration and validation.

Different approaches have been proposed to estimate marine primary production based on data from ocean color remote sensing (PP_{sat}) (Platt and Sathyendranath, 1988; Longhurst et al., 1995; Lee et al., 1996; Behrenfeld and Falkowski, 1997a; Campbell et al., 2002; Behrenfeld et al., 2005; Carr et al., 2006; Saba et al., 2010 many others). All the models consider information of the light availability at the surface or at depth, phytoplankton concentration, and a metabolic parameter related to phytoplankton photosynthesis. While the first two inputs can be routinely estimated from satellite data, the metabolic parameter can be only derived from laboratory and/or field measurements.

The most important difference among the models relies in the input that refers to the phytoplankton abundance or carbon stock (e.g., Longhurst et al., 1995; Westberry et al., 2008; Lee et al., 2011, 2015). Behrenfeld et al. (2005) and Lee et al. (1996) grouped those algorithms according to the main input: chlorophyll-a concentration (Chl) or phytoplankton carbon (C). The first type of algorithm proposed to estimate PP_{sat} uses Chl because of the primordial role that this pigment takes in the photosynthesis process (Platt and Sathyendranath, 1988; Longhurst et al., 1995; Behrenfeld and Falkowski, 1997b). The second group incorporates some information about C using the backscattering coefficient of particles (b_{bp}) (Behrenfeld et al., 2005).

A different basis is the third approach, based on phytoplankton absorption coefficient (a_{phy}, $PP_{sat-aphy-based}$) (Marra et al., 1993; Lee et al., 1996; Hirawake et al., 2011; Ma et al., 2014). Instead of biological information, this approach uses optical information. For this reason, this is the only one that uses explicitly and directly the light absorbed by phytoplankton for photosynthesis estimation, which provides not only a more intuitive understanding of C fixation through photosynthesis, but also better accuracy in estimating PP_{sat} (Lee et al., 1996, 2011; Hirawake et al., 2011). The mathematical formulation of $PP_{sat-aphy-based}$ model at depth z can be expressed as:

$$PP_{sat-a_{phy}-based}(z) = \int \phi(z) \cdot a_{phy}(z, \lambda) \cdot E(z, \lambda)\lambda \qquad (1)$$

where ϕ (mol C mol photons-1) is the quantum yield of photosynthesis, E corresponds to irradiance (measured in mol photons) for wavelength λ (nm), at depth z (m).

This ϕ is a physiological parameter that expresses the efficiency by which phytoplankton convert harvested light into oxygen released or carbon assimilated during the photosynthesis process. Then, this parameter connects light absorbed by phytoplankton to be used for photosynthesis with the rate of C fixed during photosynthesis. It links optical properties with biological information and is a key parameter for estimating PP_{sat} (Marra et al., 1993; Lee et al., 1996, 2015; Kovač et al., 2017). Presently, a_{phy} spectrum and the vertical profile of E can be well estimated from ocean color remote sensing (e.g., Lee et al., 2002, 2005b), but how ϕ changes spatially and temporally remains unknown.

Mathematically, ϕ can be described as the ratio between PP and absorbed photons (AP):

$$\phi(z) = \frac{PP(z)}{AP(z)} \qquad (2)$$

Inside the cell, photosynthesis takes place in the chloroplasts, and two photosystems are involved in this process. The light reactions in both photosystems place physiological limits on photosynthesis efficiency that confers ϕ to a maximum theoretical value of 0.125 mol C mol photons^{-1} (Iluz and Dubinsky, 2013). Actually, in nature, phytoplankton species are observed to work under much lower efficiency than this expected maximum (Morel, 1978; Marra et al., 1993; Carder et al., 1995; Sorensen and Siegel, 2001; among many others). Not only that, ϕ has been found to be subject to temporal, regional and vertical variability within the water column (Babin et al., 1996; Finenko et al., 2002; Ostrowska et al., 2012). The highest variability for different depths and different regions was reported in Ostrowska et al. (2012). In the upper water column, ϕ is ruled mainly by light levels, presenting low values at surface because of photoinhibition and higher proportion of photoprotective pigments, while higher values are found at greater depths with lower light levels, where ϕ may reach its theoretical maximum (Iluz and Dubinsky, 2013). Marra et al. (2000) quantified the effect of photoprotective pigments in ϕ.

They found that those pigments are able to reduce ϕ between 30% and 4-fold. Nutrient availability is another important factor determining ϕ value. Higher nutrient concentrations imply a higher number of active reaction centers in the photosynthetic apparatus, leading to higher photosynthetic efficiency (Kolber et al., 1998). Also, Marra et al. (2000) found that a low load of nutrients can have a secondary effect in phytoplankton cells, increasing non-photosynthetic pigment production and reducing ϕ even more. For example, clear oligotrophic waters can show lower ϕ than eutrophic areas (Morel, 1978). On seasonal time scales, however, its variation seems to be much smaller. At the global scale, and ignoring polar winter Ostrowska et al. (2012) reported a seasonal variation up to ∼1.5 times.

However, all these trends on ϕ variability depend on the physiological requirements of phytoplankton species composing the biological community and there is not an "only" factor involved in the determination of ϕ, but an interaction of all the environmental conditions (Sorensen and Siegel, 2001). This makes it extremely complicated to model ϕ accurately as a function exclusively of environmental factors without any *a priori* knowledge of the real photosynthetic efficiency at certain region. Like many other physiologically dependent parameters used in remote sensing models for PP (e.g., P^B_{opt}) (Behrenfeld and Falkowski, 1997b), the appropriate way at present to observe and model ϕ still relies on biological and optical data in different regions.

Kiefer and Mitchell (1983) found, based on laboratory measurements of daily primary production, that ϕ can be well modeled as a function of daily Photosynthetic Available Radiation (PAR_{day}),

$$\phi(z) = \phi_m \cdot \frac{K_\phi}{K_\phi + PAR_{day}(z)} \quad (3)$$

where ϕ_m is the maximum quantum yield of photosynthesis, and K_ϕ is a model parameter that represents the irradiance when ϕ corresponds to a half of ϕ_m. Hereafter, we will refer to ϕ as the instantaneous quantum yield of photosynthesis, which is then a function of light availability and a maximum parameter ϕ_m. Therefore, $PP_{sat-aphy-based}$ already takes into account the vertical variation of ϕ caused by differences in PAR at depth when using Equation 3. However, so far no application of the $PP_{sat-aphy-based}$ model considers regional and seasonal variability in ϕ caused by factors other than light, where as indicated in Iluz and Dubinsky (2013) temporal and regional varying ϕ instead of a universal factor should be employed.

To test and evaluate this strategy, we derive ϕ values in two long, *in situ* time-series, collected at fixed stations within the two North Subtropical Gyres. These stations are Hawaii Ocean Time-Series (HOT) and Bermuda Atlantic Time-series Study (BATS) and were selected because of the availability of long term and consistent pool of optical and biological data. Different from other methods that estimate the quantum yield in laboratory experiments in monospecific cultures, the approach used in this work provides the ϕ for the entire phytoplankton community subjected to natural conditions (e.g., light levels, phytoplankton community composition, nutrient concentration, pigment content, and water temperature). Because it is derived from *in vivo* conditions, its variability on time and depth takes into account photoadaptation, acclimation processes, and changes in the phytoplankton community composition as responses to changes in environmental factors. Hourly variability in ϕ is not possible since PP was measured on a daily time scale. Therefore, the derived ϕ represents mean daily photon-conversion efficiency. We are interested mainly in seasonal/regional variability in ϕ that can be directly incorporated into remote sensing applications.

Sorensen and Siegel (2001) applied a similar approach to the present study, deriving ϕ from *in situ* measurements using a few years of data at BATS. Here, however, we go beyond their findings by considering a more sophisticated approach to estimate light at depth, extending the length of the time-series, including another study area in our calculations, and utilizing remote sensing data to evaluate effectively the impact of such *in situ* ϕ in the PP_{sat} products.

Our objectives include then: (i) an observation and understanding of ϕ for both study areas, (ii) their parameterizations via taking into account its seasonal variability, and (iii) its application to a time-series of remote sensing data to obtain dynamic PP_{sat} of the two regions.

MATERIALS AND METHODS

Study Area

The datasets used in this work are public and come from the HOT (available at http://hahana.soest.hawaii.edu/hot/) and BATS (available at http://www.bios.edu/research/projects/bats/). HOT is located in the North Pacific Ocean, close to Hawaii. Data were collected in this region centered at 22°45′ N, 158°00′ W and within a radius of 6 nautical miles, at the isobaths of ∼4,000 m. The BATS station was located in the North Atlantic Ocean, centered at 31°40′ N, 64°10′ W (**Figure 1**).

Both stations are located in waters with a nutrient-limited euphotic zone. On an annual scale, nutrients are higher at surface when vertical mixing is higher, breaking the thermocline, and allowing nutrients to mix into surface waters when a shallower nitracline is observed (Bates et al., 1996; Karl et al., 1996). At HOT, these conditions are found during winter, while at BATS this period occurs in winter and extended to early spring.

The autotrophic community in both regions is dominated by small prokaryotic picoplankton, represented mainly by prochlorophyte and cyanobacteria (e.g., Platt et al., 1983; Siegel et al., 1990; Letelier et al., 1993; Sorensen and Siegel, 2001; Karl and Church, 2017).

In spite of all the environmental similarities between both stations, the primary production cycle from *in situ* measurement ($PP_{in\ situ}$) is different. Nutrients at BATS are rapidly assimilated by phytoplankton and it promotes a short spring phytoplankton bloom between January and March, when $PP_{in\ situ}$ is maximal (Menzel and Ryther, 1960; Bates et al., 1996; Sorensen and Siegel, 2001). However, this typical seasonal cycle frequently suffers inter-annual changes because of variability in winter mixed layers and surface stratification (Steinberg et al., 2001). Also, other factors such as nutrient injection via mesoscale eddies,

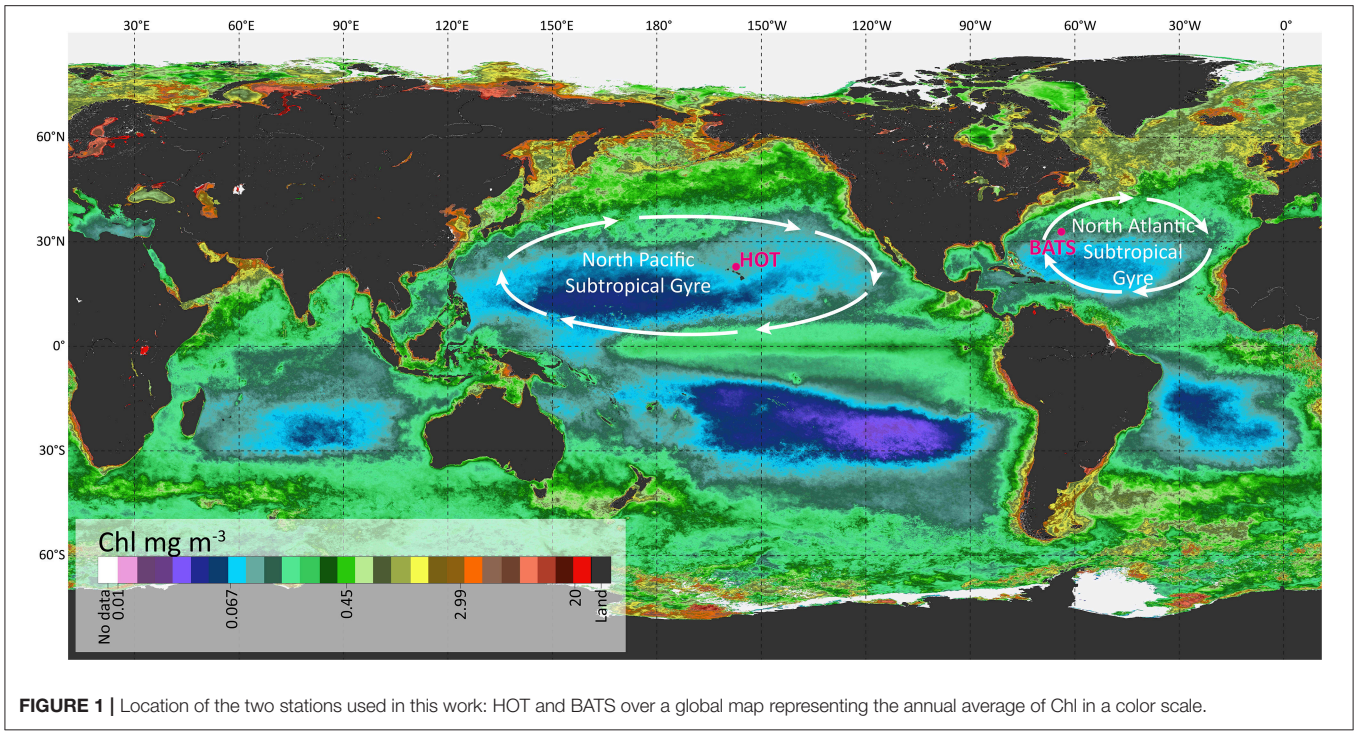

FIGURE 1 | Location of the two stations used in this work: HOT and BATS over a global map representing the annual average of Chl in a color scale.

or N_2-fixers, had been reported as responsible for seasonally anomalous phytoplankton blooms, that is, in late spring or summer (Steinberg et al., 2001). However, at BATS, such blooms are not strong enough to alter the annual carbon cycle. On the contrary, at HOT the highest $PP_{in\ situ}$ is generally found during late summer and early fall (Karl and Church, 2017), which pointed to blooms of N_2-fixers as responsible for this alteration in the $PP_{in\ situ}$ cycle and leading to a maximum in $PP_{in\ situ}$ in summer.

In situ Datasets

Data at HOT comprised *in situ* measurements collected concurrently from cruises during the period Mar/1998-Oct/2015. A total of 127 cruises at HOT were used in this work. However, only 47 cruises were found applicable for BATS for the period between Jul/1994 and Mar/2008. For both time series, sampling was conducted at monthly resolution. The protocols applied to data collection and processing are rigorously followed to guarantee consistence in the measurements over time (Sorensen and Siegel, 2001). Additional details of those protocols and collection methods can be found in their respective websites (http://hahana.soest.hawaii.edu/hot/ and http://bats.bios.edu/).

Biogeochemical Measurements

Photosynthetic production of organic matter at different discrete depths ($PP_{in\ situ}$, in mg C m^{-3} d^{-1}) was measured by the trace-metal clean ^{14}C uptake method with incubations performed *in situ* along one daylight period (dawn-to-dusk) (Fitzwater et al., 1982). In the case of HOT, the depths were 5, 25, 45, 75, 100, and 125 m; while at BATS, the depths were 1, 20, 40, 60, 80, 100, and 120 m. Light- and dark-bottles were incubated *in situ* following the same procedure and $PP_{in\ situ}$ was obtained via subtracting dark uptake from light-bottle assimilation. In the case of HOT, dark-bottle incubations were available only in the period Mar/1998-Aug/2000. These values were averaged at depth and subtracted from the light experiments after Oct/2000.

Pigment concentrations (in ng kg^{-1}) from High Performance Liquid Chromatography (HPLC) were measured the same day and at the same depths were $PP_{in\ situ}$ was estimated.

Optical Measurements

The HOT time-series performed radiometric measurements in water using two different radiometers: Profiler Reflectance Radiometer (PRR600/610, Biospherical Inc.) between March/1998 and August/2009 and Hyperpro free-falling optical profiler, from May/2009. The PRR has 6 spectral bands at 412, 443, 490, 510, 555, and 665 nm, while the Hyperpro is a hyperspectral radiometer, whose sensors measure upwelling radiance and downwelling irradiance (L_u and E_d), respectively, in the visible domain with a spectral resolution of ∼10 nm. In the case of BATS, the radiometric profiles were performed using a multispectral radiometer: Multiwavelength Environmental Radiometers (Biospherical Inc., MER-2040, San Diego, CA) up to 1999 and SeaWiFS Profiling Multichannel Radiometer and SeaWiFS Multichannel Surface Radiometer (SPMR/SMSR, Satlantic) after 1999. Those radiometers had 8 and 10 spectral bands, respectively (410, 441, 465, 488, 520, 565, 589, and 665 nm in the case of 8-bands, and additionally at 625 and 683 nm for the 10-bands radiometer). In all the cases, at the same time that the in-water measurements were registered, a radiometer installed above-surface took measurements of solar irradiance (E_S), which were used to correct $E_d(z)$ from cloud effects. The

E_d measurements were taken the same day or within one day of difference respect the $PP_{in\ situ}$ experiment.

Measurements of solar $PAR_{in\ situ}$ (in μmol photons m^{-2} s^{-1}) above surface were registered dawn-to-dusk during the day of $PP_{in\ situ}$ experiments using a LI-COR LI-1000 integrator/datalogger that registers flux of photons between 400 and 700 nm.

Phytoplankton absorption coefficient ($a_{phy,in\ situ}(\lambda)$) at BATS was estimated during the whole time series following the NASA protocols (NASA, 2003). Seawater was filtered using Whatman GF/F glass fiber filter pads, which were kept frozen in liquid nitrogen until readings (Morrison and Nelson, 2004). Absorption of the filter pad was measured before and after pigment extraction with methanol (Kishino et al., 1985). $a_{phy,in\ situ}(\lambda)$ was estimated as a difference between total absorption (before bleaching) and detritus absorption (after bleaching). At HOT, $a_{phy,in\ situ}(\lambda)$ was reconstructed by the pigment concentration measured by HPLC (Bidigare et al., 1990; Marra et al., 2000). In this case, it used the unpackaged specific absorption spectra derived from Gaussian approximations and applied the package effect correction available in Wozniak et al. (1999).

Satellite Datasets

Data collected by the MODIS-Aqua sensor between Jul/2002-Dec/2014 were used. The data was downloaded in Level-3 Standard Mapped Image Products, 8-Day composite, in 4-km spatial resolution (https://oceancolor.gsfc.nasa.gov/). Also acquired were the following standard products: Sea Surface Temperature (SST_{sat}, in °C); Daily Photosynthetically Available Radiation ($PAR_{day,sat}$, in mol photons m^{-2} d^{-1}) (Frouin et al., 1989); absorption coefficients due to phytoplankton and due to gelbstoff and detrital material at 443 nm [$a_{phy,sat}(443)$ and $a_{dg,sat}(443)$, respectively, in m^{-1}]; particulate backscattering at 443 nm [$b_{bp,sat}(443)$, in m^{-1}]. All the acquired Inherent Optical Properties [$a_{phy,sat}(443)$, $a_{dg,sat}(443)$ and $b_{bp,sat}(443)$] were estimated through the Generalized Inherent Optical Property (GIOP) model (Werdell et al., 2013). The spectral parameters ($S_{adg,sat}$, in nm^{-1}, and $S_{bb,sat}$, respectively) required for the derivation of these absorption and backscattering coefficients were processed as in the Quasi-Analytical Algorithm (QAA, Lee et al., 2002). These products were extracted within a 3 × 3 pixel window centered at the geographical coordinates of HOT and BATS stations, average of this window is further estimated for each product to comprise satellite time series between 2002 and 2014.

Data Processing

In situ Data Processing: $PP_{in\ situ}$

At HOT, $PP_{in\ situ}$ was obtained from *in situ* experiments from Mar/1989 to Oct/2015, while at BATS it was from Jul/1989 to Dec/2016. The integration in the euphotic zone was performed through the trapezoid method (Saba et al., 2010) and included the depths detailed in section Biogeochemical Measurements for both regions.

In situ Data Processing: PAR_{day} (λ)

The processing to obtain $PAR_{day,in\ situ}(z, \lambda$, expressed in mol photons m^{-2} s^{-1} nm^{-1}) is summarized in the flow-chart in **Figure 2**.

1) Simulations in Hydrolight (Mobley and Sundman, 2008) were run to estimate $E_S(\lambda)$ in different conditions that affect solar irradiance at the surface, such as solar zenith angle (0, 30, and 60°), atmospheric visibility (15 and 40 km), cloud percentage (10, 20, 50, 80, and 100%), atmospheric humidity (20, 80, and 100), and atmospheric ozone content (200 and 400). We integrated $E_S(\lambda)$ (W m^{-2}) in the visible domain [E_S(PAR), W m^{-2}] and calculated the normalized spectra $\overline{E}_S(\lambda)$ as $\overline{E}_S(\lambda) = \frac{E_S(\lambda)}{E_S(PAR)}$. $\overline{E}_S(\lambda)$ showed a shape well preserved along all the atmospheric conditions tested, with only small differences <8%, toward the blue and red regions. Then we used $\overline{E}_S(\lambda)$ to spectrally resolve $PAR_{in\ situ}$ recorded by LI-COR, by simple multiplication between each LI-COR measurement and $\overline{E}_S(\lambda)$ [see $\overline{E}_S(\lambda)$ in the **Appendix**]. In this way, we obtained light variability above surface, and spectrally resolved $PP_{in\ situ}$ over a day [$PAR_{in\ situ}(0^+,\lambda,t)$].
2) $PAR_{in\ situ}(0^+,\lambda,t)$ was integrated spectrally and along the day to obtain $PAR_{day,in\ situ}(0^+)$ which was used further in section Dynamic temporal parameterization of ϕm and K_ϕ.
3) To estimate $PAR_{in\ situ}(\lambda)$ at depth, information about light attenuation is needed. Considering that both stations are located in oligotrophic areas, where water dominates light attenuation for wavelengths >560 nm, and that E_d profiles in wavelengths longer than 560 nm were very noisy, we took the diffuse attenuation coefficient in the range of 561–700 nm [$K_{d,in\ situ}$(561–700), m^{-1}] equal to the K_d for pure seawater ($K_{d,pure\ water}$). For the wavelengths between 400 and 560 nm, two different processing routines were applied to obtain $K_{d,in\ situ}(\lambda)$, according to the type of radiometer used in each cruise (multi- or hyper-spectral).
4) In the case of hyper-spectral data, K_d(400–560) was obtained from $\hat{E}_{d,in\ situ}(z, \lambda)$ profiles (Zoffoli et al., 2017), where $\hat{E}_{d,in\ situ}(z, \lambda)$ represents measured downwelling spectral irradiance.
5) In the case of multispectral information, the following pertain:
   a. The above-water remote sensing reflectance [$Rrs_{in\ situ}(0^+, \lambda)$, in sr^{-1}] was obtained from the profiling measurements following NASA protocol (NASA, 2003) and corrected from Raman effects (Lee et al., 2013).
   b. Raman-corrected $Rrs_{in\ situ}(0^+, \lambda)$ was used as input for the QAA v6 algorithm (Lee et al., 2002; Lee, 2014) to obtain $a_{phy}(443)$, $a_{dg}(443)$, and $b_{bp}(555)$. Along with the spectral parameters S_{adg} and S_{bb}, these properties were used to generate hyperspectral a_{phy}, a_{dg}, and b_{bp} as in HOPE (Lee et al., 1999).
   c. Spectra of total absorption and backscattering coefficients were thus calculated as sum of these components, and then K_d(400–560) was estimated following Lee et al. (2005a), Lee et al. (2013). Being an Apparent Optical Property (AOP), K_d changes with light field. In the above estimation, the

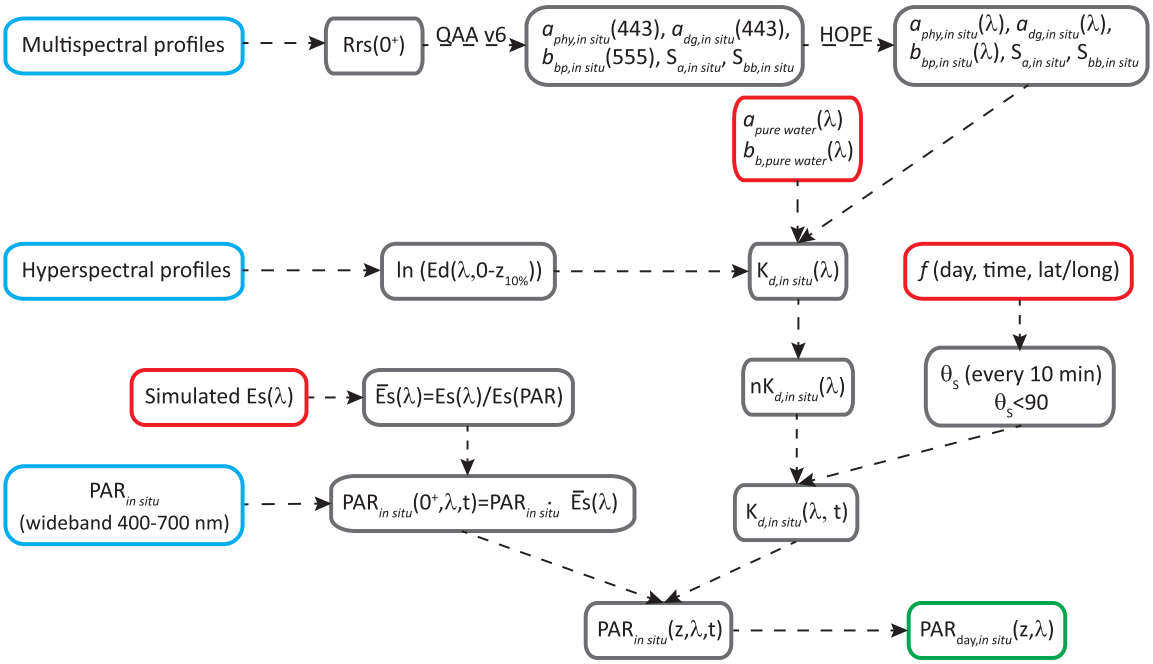

FIGURE 2 | Flow-chart to obtain daily PAR ($PAR_{day,in\ situ}$) from *in situ* data.

change of solar zenith angle (θ_s) was also incorporated, where θ_s was determined based on information of location, day of the year and time of the day.

6) $PAR_{in\ situ}(0^-,\lambda,t)$ together with the $K_d(\lambda,t)$ allowed the estimation of the irradiance at different depths, every 10 min, for the visible domain [$PAR_{in\ situ}(z,\lambda,\ t)$] as $PAR_{in\ situ}(z,\lambda,t) = PAR_{in\ situ}(0^-,\lambda,t)\cdot e^{-K_d(\lambda,t)z}$
7) Finally, $PAR_{day,in\ situ}(z,\lambda)$ was estimated by integration of $PAR_{in\ situ}(z,\lambda,t)$ between initial and final time of the incubation (sunrise and sunset, respectively).

In situ Data Processing: ϕ

For each region, cruise, and depth, instantaneous ϕ was estimated from $PP_{in\ situ}(z)$ and $PAR_{day,in\ situ}(z,\lambda)$ following:

$$\phi(z) = \frac{PP_{in\ situ}(z)}{\int_{400}^{700} a_{phy}(\lambda,z)\cdot PAR_{day,\ in\ situ}(z,\lambda)\lambda} \quad (4)$$

In this approach, $a_{phy}(\lambda,z)$ was considered constant over the whole day.

ϕ_m and K_ϕ were further calculated for every cruise/station using the coefficients from a linear fitting of the semi-log graph $\ln[\phi(z)]$ vs. $PAR_{day,in\ situ}(z)$, where the offset corresponded to $\ln(\phi_m)$. Then, for each cruise, K_ϕ was estimated as value of $PAR_{day,in\ situ}$ for ϕ equals $\phi_m/2$.

Dynamic Temporal Parameterization of ϕ_m and K_ϕ

From the values derived above, monthly ϕ_m and K_ϕ were calculated and smoothed for HOT and BATS. ϕ_m was described as a linear function of the ratio between sea surface temperature (SST) and 20 (SST/20). The value of 20 was chosen as the optimum temperature for carbon fixation and as explained in the discussion. K_ϕ was modeled as a linear function of $PAR_{in\ situ}(0^+)$. The results of such parameterization are presented in section Quantum yield of photosynthesis and dynamic parameterizations of ϕm and K_ϕ. After incorporating monthly SST or PAR data obtained from satellite, empirical relationships were developed that well describe the variation of ϕ_m and K_ϕ.

Satellite Data Processing

PP_{sat} in this work was estimated via two different approaches, with one using the conventional Chl-based scheme ($PP_{sat-chl-based}$), while the other using the a_{phy}-based scheme. For both HOT and BATS, the waters were considered homogeneous in the distribution of water constituents. In the case of $PP_{sat-chl-based}$, the VGPM system (Behrenfeld and Falkowski, 1997b) was used to estimate primary production. In this case, PP_{sat} is estimated as the integral in the euphotic zone according to Equation 5:

$$PP_{sat-chl-based} = 0.66125\cdot P^B_{opt}\cdot\frac{PAR_{sat}(0^+)}{(PAR_{sat}(0^+)+4.1)}\cdot z_{eu}\cdot Chl_{sat}\cdot D \quad (5)$$

where P^B_{opt} is the maximum carbon fixation rate within the water column (mg C mg Chl^{-1} h^{-1}), D is day length (in hour) and Chl_{sat} is the chlorophyll concentration obtained from satellite data. Following Behrenfeld and Falkowski (1997b), P^B_{opt} was modeled based on SST. We acquired $PP_{sat-chl-based}$ from the

Ocean Productivity Home Page (Oregon University) for 8-Day composites in 9 km of spatial resolution between 2002 and 2014. A 1 × 1 pixel window was extracted centered in each station coordinates.

The model proposed by Kiefer and Mitchell (1983) was used to obtain the variation of ϕ caused by light intensities (Equation 3). Here we estimated the integral of PP_{sat} (Equation 6) for the euphotic zone to be comparable with $PP_{sat-chl-based}$ values. We considered z_{eu} as 125 m for HOT and 120 m for BATS.

$$PP_{sat-a_{phy}-based} = \int_0^{zeu} \int_{400}^{700} \phi(z) \cdot a_{phy,sat}(\lambda) \cdot PAR_{day,sat}(z,\lambda)\, d\lambda dz \quad (6)$$

As in section *in situ* data processing: $PP_{in\ situ}$ for processing multispectral data, $a_{phy,sat}(\lambda)$ was calculated as a function of

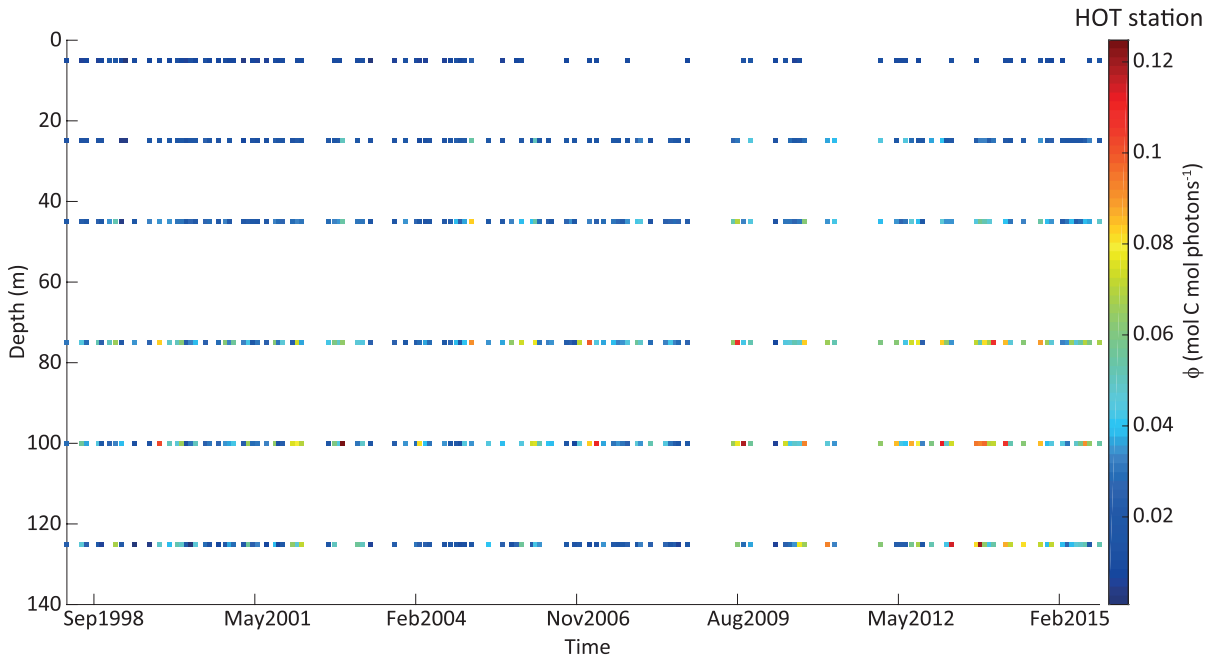

FIGURE 3 | Quantum yield of photosynthesis (ϕ, in mol C mol photons $^{-1}$) estimated from *in situ* measurements at HOT station, represented in a colorimetric scale (exhibited on the right). The vertical axis shows the depth in meters (from 0 on the top to deeper values on the bottom). The horizontal axis represents time and every point in the graph corresponds to a monthly cruise.

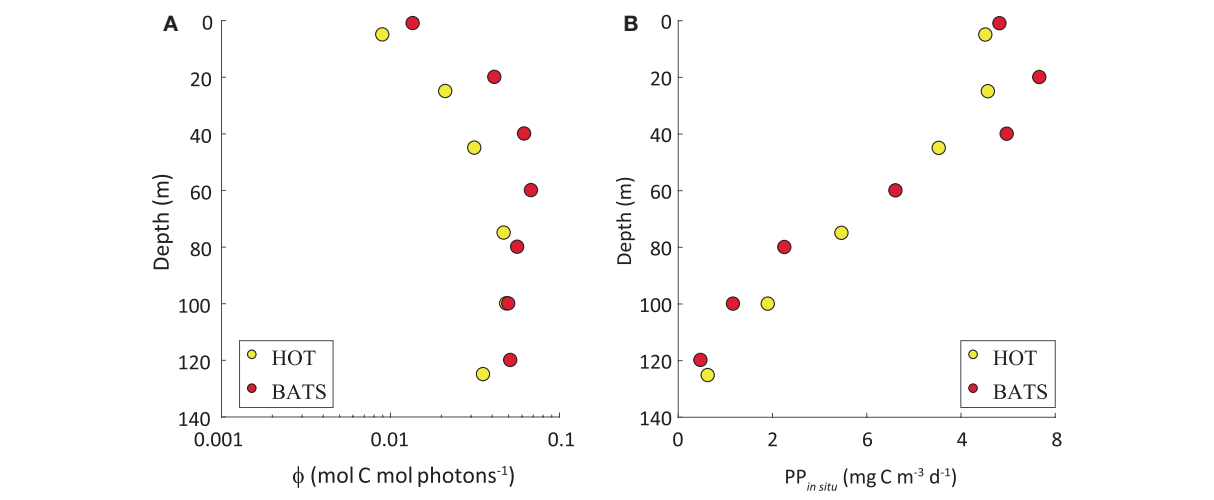

FIGURE 4 | (A) Annual average of the quantum yield of photosynthesis (ϕ, in mol C mol photons $^{-1}$) in a vertical scale. The abscissa axis represents ϕ exhibited in log-scale (mol C mol photons^{-1}) and the ordinate axis shows depth (in m). **(B)** $PP_{in\ situ}$ (mg C m^{-3} d^{-1}) along the water column. In both graphs, yellow dots represent HOT and red dots, BATS.

$a_{phy,sat}(443)$ following the HOPE model (Lee et al., 1999). Starting from $PAR_{day,sat}$, we obtained a $PAR_{day,sat}(\lambda)$ by simple multiplication of PAR_{sat} and the normalized spectrum $\overline{E}_S(\lambda)$. $K_{d,sat}$ for the average daily zenith angle of each 8-Day composite was used to estimate the $PAR_{day,sat}$ at depth, where $PAR_{day,sat}(z,\lambda) = PAR_{day,sat}(0^-,\lambda) \cdot e^{-Kd(\lambda)\cdot z}$. Again, following Lee et al. (2005a, 2013), $K_{d,sat}$ was calculated from the derived total absorption and backscattering coefficients. The values of ϕ_m and K_ϕ were derived previously in section Dynamic temporal parameterization of ϕ m and Kϕ, and $\phi(z)$ at depth was calculated as Equation 3.

Method to Evaluate Performance

The satellite and *in situ* datasets cover different time spans. About 26 years of data comprise the $PP_{in\ situ}$ data while ~12 years were collected by satellites. Also, the data sampling was performed at different time intervals. *In situ* experiments lasted one day in ~monthly intervals, while here we used satellite products on an 8-Day composite basis. Not only temporal sampling is different, but also spatial resolution is significantly different. While *in situ* data came from experiments performed at one location, satellite data came from an integrated area of 9 × 9 km^2 in the case of $PP_{sat-chl-based}$ and 4 × 4 km^2 for $PP_{sat-aphy-based}$. For these reasons, rather than a match-up exercise, we wanted to evaluate whether PP_{sat} is able to reproduce the overall magnitude and seasonal variations observed in $PP_{in\ situ}$. Therefore, differences between monthly median *in situ* PP ($\hat{P}P_{in\ situ}$) and monthly PP_{sat} ($\hat{P}P_{sat}$) were measured using Unbiased Absolute Percent Difference (UAPD) (Equation 7):

$$UAPD\ (\%) = 2 \cdot |(\hat{P}P_{in\ situ} - \hat{P}P_{sat})| \Big/ (\hat{P}P_{in\ situ} + \hat{P}P_{sat}) \cdot 100 \quad (7)$$

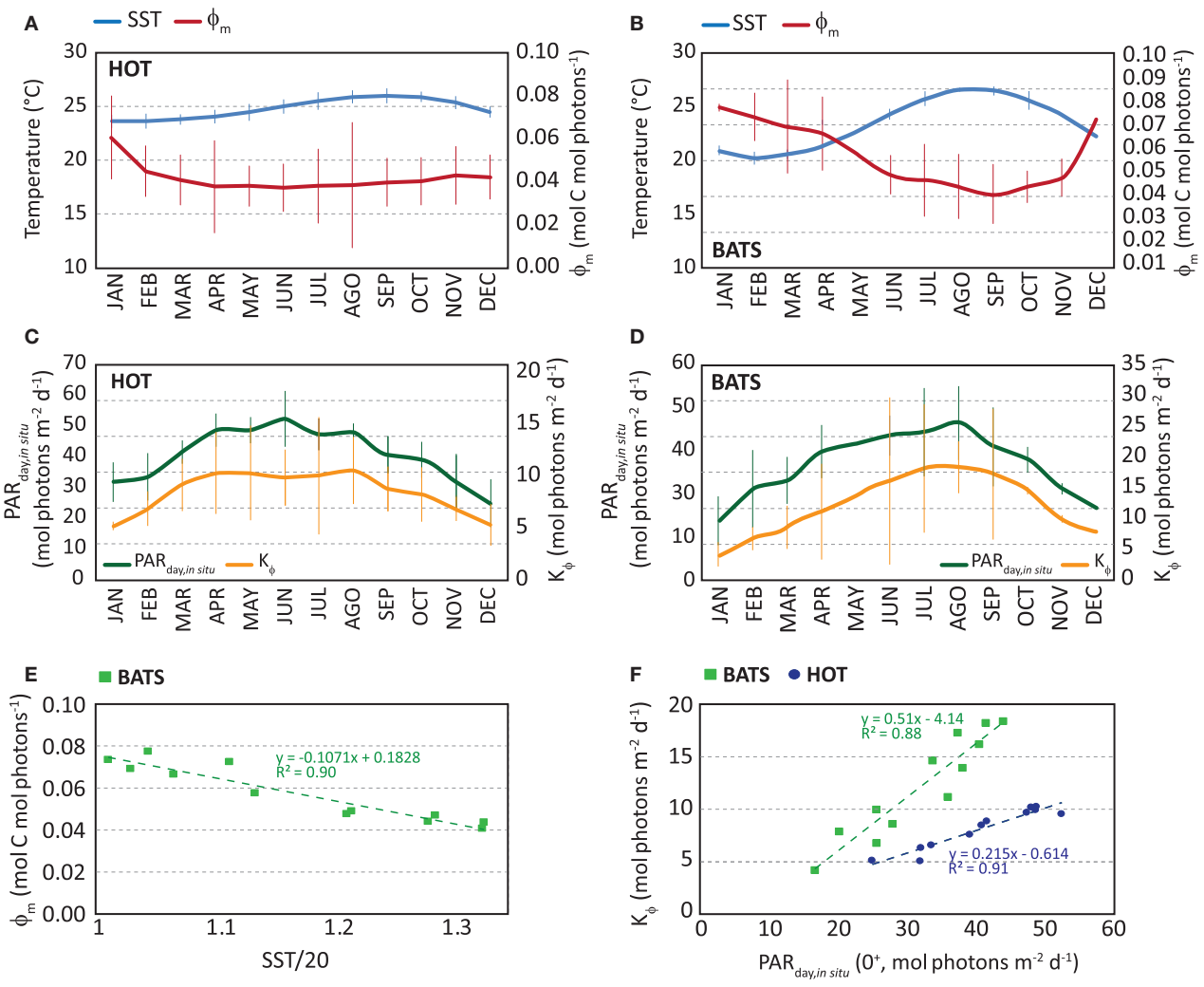

FIGURE 5 | Monthly median of *in situ* maximum quantum yield of photosynthesis (ϕ_m, in mol C mol photons $^{-1}$) in red and *in situ* monthly median of sea surface temperature (SST, in °C) in blue: **(A)** at HOT and **(B)** at BATS. Error bars represent standard deviation. Monthly median of *in situ* K_ϕ (in mol photons m^{-2} d^{-1}) in yellow and *in situ* monthly median of $PAR_{day,in\ situ}$ (in mol photons m^{-2} d^{-1}) in green: **(C)** at HOT and **(D)** at BATS. Error bars represent standard deviation. **(E)** *In situ* monthly median ϕ_m as a function of monthly SST at BATS and **(F)** *in situ* monthly median K_ϕ as a function of $PAR_{day,in\ situ}$ (0$^+$). In graph and **(F)** results of both stations are displayed together, where HOT is represented by blue circles and BATS as green squares.

RESULTS

Quantum Yield of Photosynthesis and Dynamic Parameterizations of ϕ_m and K_ϕ

The derived instantaneous ϕ showed a large range of variability at both stations along the time series and within the water column (**Figure 3**). Within the period used at BATS (14 years), we had many gaps with incomplete cruise datasets. For this reason, we do not show the timeline for this station. At HOT, minimum and maximum values were ∼0.001 and 0.126 mol C mol photons^{-1}, respectively, and corresponded to more than 120-fold of variability. However, more than 95% of the cases were lower than 0.07 mol C mol photons^{-1}, which reduced the variability to 69-fold. A slightly lower range was presented at BATS (∼0.002–0.121 mol C mol photons^{-1}), which corresponded to 50-fold of variability. Restricting instantaneous ϕ to 95% of the occurrences, it varies in a range of ∼0.002–0.1 mol C mol photons^{-1}, reducing its variability to 45-fold.

As expected, the highest variability in the ϕ was observed vertically, with the lowest values at the surface and the highest at depth (**Figure 4A**). This pattern was opposite to the vertical distribution of $PP_{in\ situ}$ (**Figure 4B**). While $PP_{in\ situ}$ is ruled mainly by light availability, the highest efficiencies are found at deeper depths. The maximum values of the instantaneous ϕ in both stations almost attained the maximum theoretical value and they were observed at great depths with very low light levels. On some cruises, the ϕ obtained at the greatest depths surpassed the theoretical maximum of 0.125 mol C mol photons^{-1}. At those depths, both $PP_{in\ situ}$ and light levels are very low, thus potentially creating very high uncertainties in the estimated ϕ due to difficulties in obtaining accurate $PP_{in\ situ}$ and light intensity at such low values. Therefore, any ϕ values higher than 0.125 mol C mol photons^{-1} were omitted and we have ignored depths >80 m to avoid estimations subjected to high uncertainties.

We observed a consistent seasonal variability in the instantaneous ϕ in both stations during the whole time series. Also, *in situ* ϕ_m and K_ϕ showed temporal variabilities. At HOT, higher ϕ_m values were found during winter (Jan–Feb), but the range of variability is quite narrow (monthly median is 0.038–0.045 mol C mol photons^{-1} except January) (**Figure 5A**). Instead, at BATS, the highest ϕ_m was observed for a longer season, from Fall to Winter (Oct–Mar), with a higher seasonal variability (monthly median 0.050–0.096 mol C mol photons^{-1}) (**Figure 5B**). According to previous works (e.g., Bates et al., 1996), the higher photosynthetic efficiency found in Fall-Winter can be related to the position of the thermocline and, therefore, to injection of nutrients into the euphotic zone. In both regions, between Summer and Spring the photosynthetic efficiency remained low.

On the other hand, K_ϕ is found following the temporal variability of $PAR_{day}(0^+)$, with the highest values in Summer and the lowest in Winter (**Figures 5C,D**). Comparing both stations, a higher annual median value was observed in ϕ_m at BATS, suggesting a higher photosynthetic efficiency during the whole year. K_ϕ was higher at BATS as well. Also at BATS, the monthly variability in the parameters was found higher than HOT, even though both stations were located in oligotrophic waters of the North Subtropical Gyres. Estimated median annual values of ϕ_m were 0.0395 and 0.063 mol C mol photons^{-1} at HOT and BATS, respectively; while K_ϕ values were 8.0 and 10.8 mol photons m^{-2} d^{-1}, respectively. The seasonal patterns found in both parameters and stations led us to incorporate temporal variation in the model through a

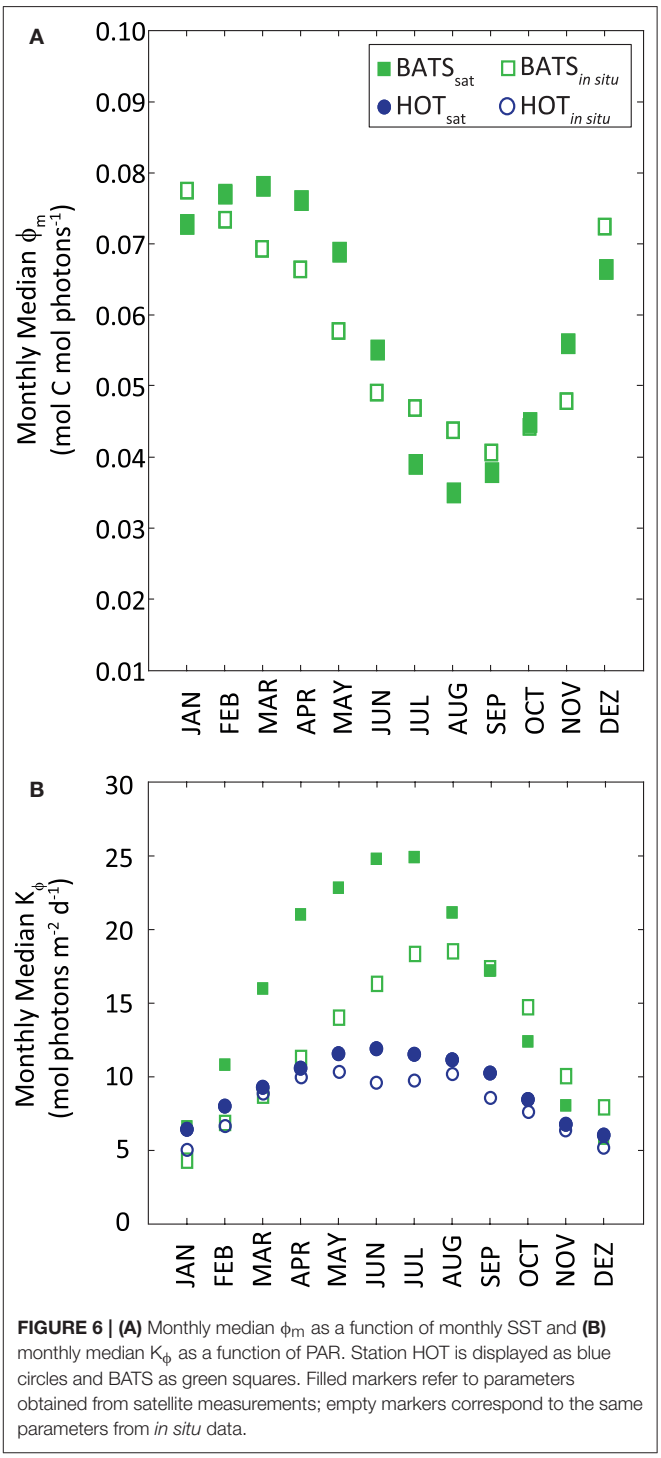

FIGURE 6 | (A) Monthly median ϕ_m as a function of monthly SST and **(B)** monthly median K_ϕ as a function of PAR. Station HOT is displayed as blue circles and BATS as green squares. Filled markers refer to parameters obtained from satellite measurements; empty markers correspond to the same parameters from *in situ* data.

dynamical modeling of ϕ_m and K_ϕ, (**Figures 5E,F**) as presented below:

$$\phi_m = -0.0451 \cdot \left(\frac{SST}{20}\right) + 0.098,$$

$$\text{and } \phi_m \leq 0.125 \text{ mol C mol photons}^{-1} \quad (8)$$

$$K_\phi = 0.215 \cdot PAR_{day,in\ situ}\left(0^+\right) - 0.614 \quad (9)$$

$$\phi_m = -0.1071 \cdot \left(\frac{SST}{20}\right) + 0.1828,$$

$$\text{and } \phi_m \leq 0.125 \text{ mol C mol photons}^{-1} \quad (10)$$

$$K_\phi = 0.51 \cdot PAR_{day,in\ situ}\left(0^+\right) - 4.14 \quad (11)$$

Here, Equations 8, 9 correspond to parameterizations for ϕ_m and K_ϕ at HOT (regression analysis for ϕ_m vs. (SST/20): $R^2 = 0.17$, $p = 0.183$, for K_ϕ vs. PAR: $R^2 = 0.91$, $p = 1.7\ 10^{-6}$, at 95% confidence level); while Equations 10-11 are used at BATS (regression analysis for ϕ_m vs. (SST/20): $R^2 = 0.90$, $p = 2.89\ 10^{-6}$, for K_ϕ vs. PAR: $R^2 = 0.88$, $p = 8.22\ 10^{-6}$, at 95% confidence level). The *p*-values suggest significance in models, except for the quadratic relation between ϕ_m and (SST/20) at HOT. The narrow variability not only in monthly ϕ_m but also in SST, explains its lack of significance in the parameterization for HOT. For this reason, we did not incorporate this parameterization into the instantaneous ϕ modeling but decided to keep it constant and equal to the median annual value (0.0395 mol C mol photons^{-1}).

Median values of ϕ_m and K_ϕ resulted from the above modeling were similar to those found *in situ*, even when they were derived from different inputs and slightly different periods of time (**Figure 6**). Median ϕ_m was 0.060 mol C mol photons^{-1} at BATS. K_ϕ resulted in 9.5 mol photons m^{-2} d^{-1} at HOT and higher at BATS (15.7 mol photons m^{-2} d^{-1}). At BATS, the modeled ϕ_m from SST_{sat} showed higher values in Fall-Winter and the lowest in Summer, following the *in situ* pattern. Sorensen and Siegel (2001) found a similar relationship between ϕ_m and SST at BATS. Even though the correlation was weak, it seems that SST is a good predictor for ϕ_m over the year, thus allowing an effective temporal modeling of ϕ_m. The temporal pattern of K_ϕ modeled with $PAR_{day,sat}$, was the same as that observed *in situ* at the two stations.

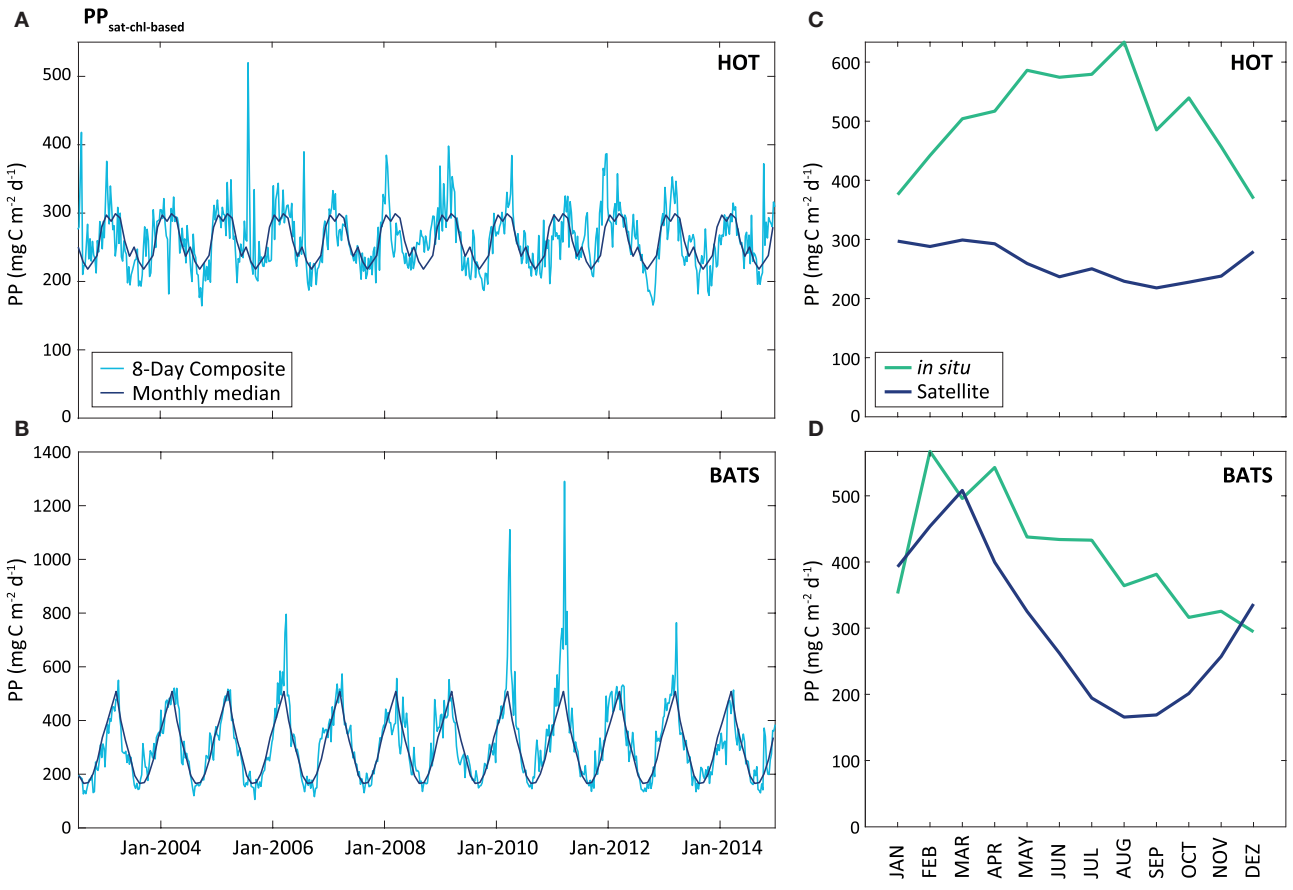

FIGURE 7 | PP_{sat} (expressed in mg C m^{-2} d^{-1}) obtained through the VGPM model, Chl-based. The light blue line represents the results obtained for the 8-Day composite, while the dark blue represents the monthly median calculated for these data, at HOT **(A)** and BATS **(B)**. The graphs on the right shows a comparison between satellite and *in situ* PP estimates (monthly median of the $PP_{sat-chl-based}$ in the blue line, and monthly median of the $PP_{in\ situ}$ in the green line), for HOT **(C)** and BATS **(D)**.

PP by Satellite

Comparing $PP_{sat-chl-based}$ with $PP_{in\ situ}$, the performance by the default VGPM for the two stations is different (**Figure 7**). At HOT, the $PP_{sat-chl-based}$ presented a strong underestimation with average difference of 62.8%, and a seasonal pattern opposite to *in situ* measurements ($R^2 = 0.27$). At BATS, the performance was better than that at HOT, with mean AUPD of 37.8%. At BATS the seasonal cycle was similar to that of *in situ* measurements ($R^2 = 0.34$), but with a delay of 3–4 months in the minimum and a shorter length on the maximum.

On the contrary, the $PP_{sat-aphy-based}$ model with the dynamic parameterization of ϕ considerably reduces the differences between satellite estimates and *in situ* measurements at HOT. In this area, UAPD reduced to only 8.3%. At BATS, UAPD remains about the same (36.4%). However, results are improved when observing the seasonal pattern. $PP_{sat-aphy-based}$ is able to well reproduce the PP seasonal cycle in both areas ($R^2 = 0.76$ at HOT; $R^2 = 0.71$ at BATS, **Figure 8**). The summer maximum of $PP_{sat-aphy-based}$ matches the *in situ* findings. The overestimation of the PP peak at BATS still needs to be inspected. Interestingly, the highest instantaneous ϕ, which is a function of both ϕ_m and K_ϕ, does not correspond to the maximum PP at HOT (**Figure 9**). Even when the ϕ is highest in winter, the PP peak was predicted to be during summer. The quantum yield of photosynthesis is not exclusively nutrient-driven nor light-driven but a combination of both factors (Sorensen and Siegel, 2001), which explains its large temporal variability. However, it is important to keep in mind that the instantaneous ϕ is not the only parameter responsible for PP, but also the phytoplankton absorption (which is related to its abundance) and light availability. Note that even though the temporal pattern of $PP_{in\ situ}$ is different, both PAR and a_{phy} showed a similar seasonal variation comparing both stations (**Figure 10**). We also run the $PP_{sat-aphy-based}$ model using annual median values of ϕ_m and K_ϕ instead of the dynamic parameterization, as a way to evaluate the impact of the temporal variability in those parameters on predicting PP. In this case, at HOT the temporal response of PP generally followed the *in situ* values with lower correlation ($R^2 = 0.70$) (**Figure 8C**, red curve), and slightly lower performance in terms of magnitude, with AUPD of 9.1%. At BATS, however, using fixed parameters

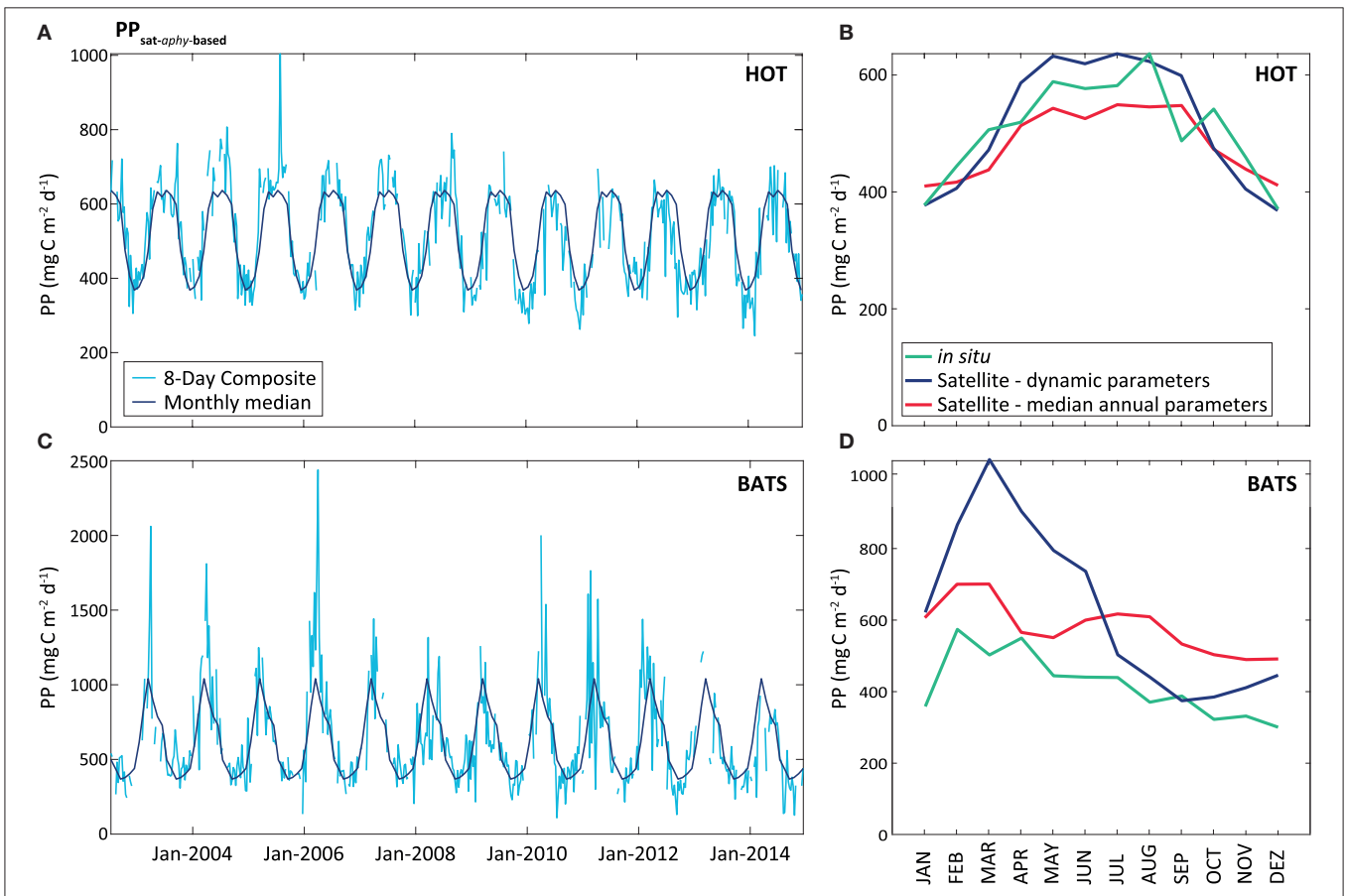

FIGURE 8 | PP_{sat} (expressed in mg C m^{-2} d^{-1}) obtained through the a_{phy} model using temporal dynamic parameterization. The light blue line represents the results obtained for the 8-Day composite, while the dark blue represents the monthly median calculated for these data, at HOT **(A)** and BATS **(B)**. The graphs on the right shows a comparison between satellite and *in situ* PP estimates (monthly median of the $PP_{sat-aphy-based}$ using our dynamic parameterization in the blue line, monthly median of the $PP_{sat-aphy-based}$ using both parameters as constant in the red line, and monthly median of the $PP_{in\ situ}$ in the green line), for HOT **(C)** and BATS **(D)**.

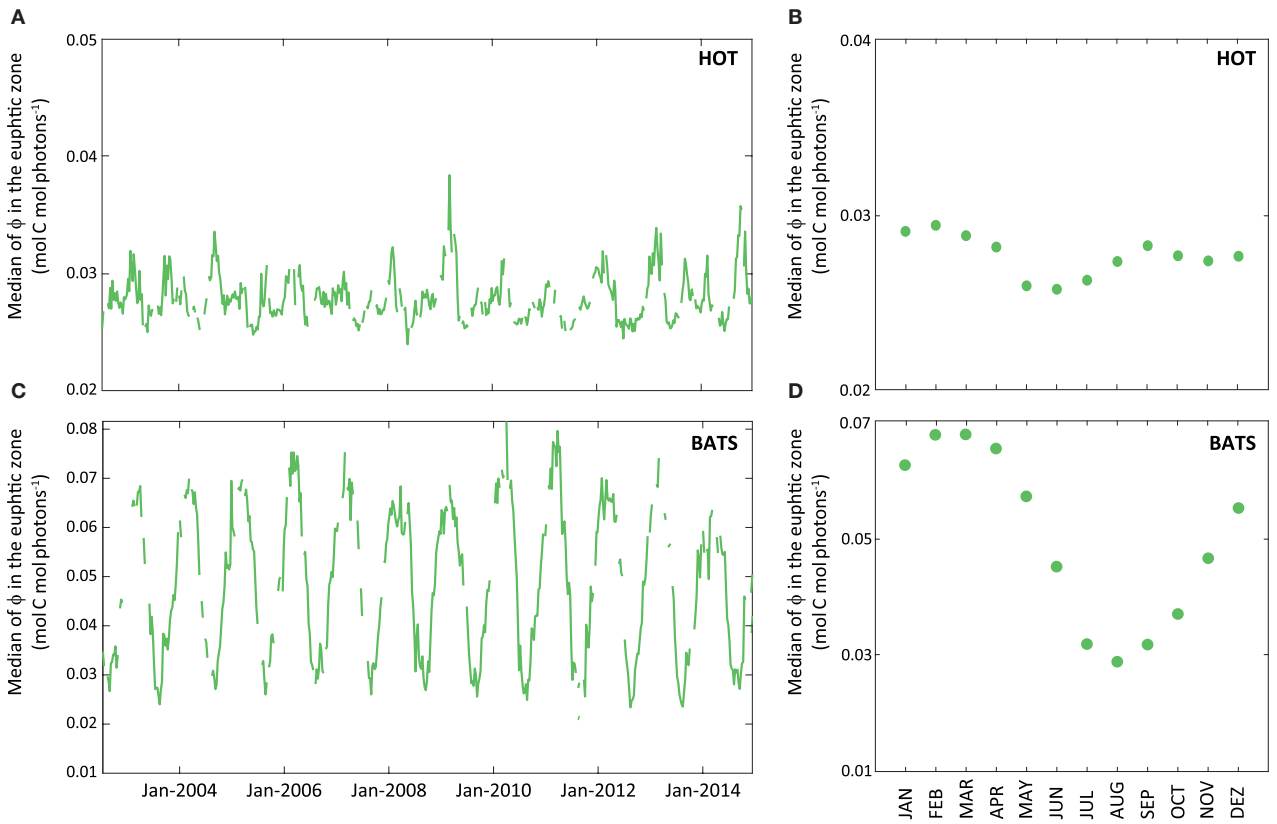

FIGURE 9 | Average of instantaneous ϕ (expressed in mol C mol photons^{-1}) within the euphotic zone obtained through MODIS-Aqua data for the whole data series (2002–2014). The green line represents the median of instantaneous ϕ for the euphotic zone **(A)** at HOT and **(B)** BATS. Aside, graphs **(C)** and **(D)** show the monthly median of ϕ for each of the stations obtained from satellite.

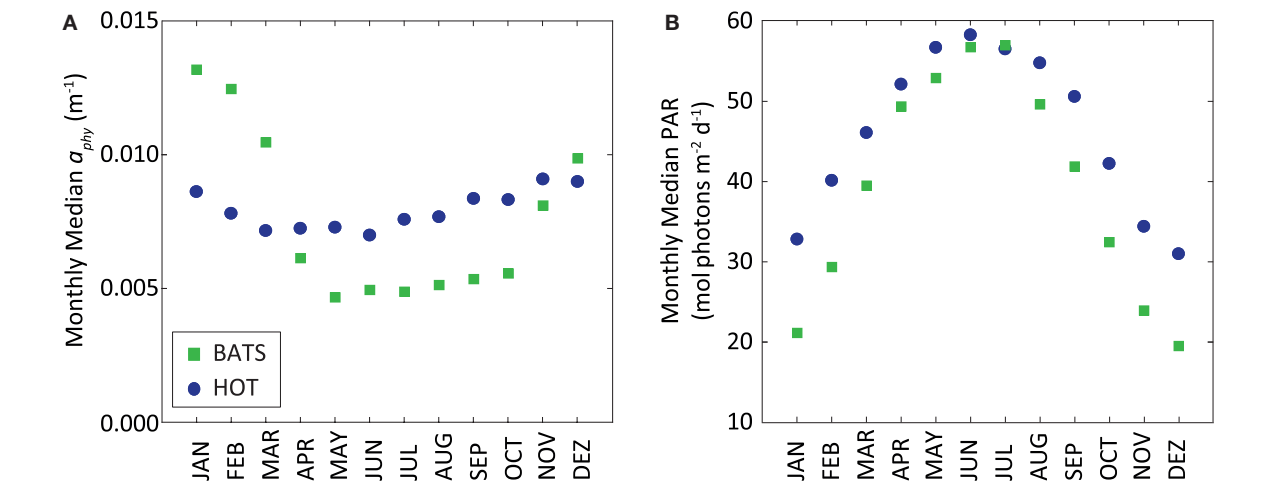

FIGURE 10 | (A) Monthly median of MODIS-Aqua a_{phy} (m^{-1}) and **(B)** monthly median of MODIS-Aqua PAR (mol photons m^{-2} d^{-1}) at surface. In both graphs stations HOT (blue circles) and BATS (green squares) are displayed together.

PP showed a similar AUPD (35.2%) but a worse response in terms of the seasonal pattern ($R^2 = 0.53$) with a secondary peak of PP during summer not observed *in situ* (**Figure 8D**, red curve). These findings support then the need of regional *in situ* measurements and incorporating temporal dependence on photosynthetic parameters according to the study area. It is

exactly the efficiency in the conversion from light into fixed C (this is the ϕ) that conforms satellite measurements into the real environmental observations, and thus fixed values for ϕ_m and K_ϕ would limit the capability to produce consistent observations for the global oceans.

DISCUSSION

In this work, we estimated ϕ_m and K_ϕ from *in situ* measurements. According to their temporal behavior, we modeled ϕ_m and K_ϕ based on *in situ* measurements as function of environmental parameters. At HOT, *in situ* median value of ϕ_m was equal to 0.04 mol C mol photons^{-1}. While at BATS, annual median values of ϕ_m were found between ∼0.06 mol C mol photons^{-1} from both methods. K_ϕ varied between 8 and 16 mol photons m^{-2} d^{-1} for both, stations and methods. These magnitudes are in good agreement with such values provided in other works. Kiefer and Mitchell (1983) found ϕ_m as 0.06 mol C mol photons^{-1} and K_ϕ as 10 mol photons m^{-2} d^{-1} from laboratory analysis using monocultures of a diatom species and varying nutrient and light levels. Morel (1978) estimated ϕ_m in the Sargasso Sea from *in situ* measurements and found an average of 0.03 mol C mol photons^{-1}. In a work developed at BATS from the same dataset (Sorensen and Siegel, 2001), it was found an average ϕ_m ∼0.035 mol C mol photons^{-1}. This value is slightly lower than the values presented in this work, but in this case the same seasonal pattern with the lowest ϕ_m in summer. Also in the referred work, K_ϕ was 16 mol photons m^{-2} d^{-1}, a bit higher than that obtained here. These differences can be caused by differences in the time period used in both works and the inputs [a_{phy} and $E_d(z)$] used to derive those parameters. Morel (1978) considered only two cruises (in May/1970 and March-April/1974 totalizing 32 stations) and Sorensen and Siegel (2001) used only 5 years of data. We included 14 years of measurements.

The dynamic parameterization we adopted was SST_{sat} for the estimation of ϕ_m at BATS and $PAR_{day}(0^+)$ for K_ϕ in the two regions. It is known that phytoplankton have an optimum temperature for growth and photosynthesis (Li, 1980). Lower temperatures mean physiological restrictions in the metabolism of the Calvin Cycle (Falkowski, 1980). Above such an optimum, there are also metabolic restrictions linked to protein inactivation and denaturation (Ratkowsky et al., 1983). **Figure 11** illustrates the P^B_{opt} parameter, used by the VGPM. This parameter shows the maximum C fixation rate within a water column, and is obtained from a polynomic function that depends only on SST. It expresses the metabolic functioning of phytoplankton and we use it here to show the relation between temperature and physiology. Note that SST_{sat} in this region in the period 2002–2014 ranges within narrow intervals:18–28.8°C, and the optimum temperature seems to be ∼20°C and not at the highest values observed. Besides physiology, temperature and nutrient inputs could also be related in the euphotic zone. Even though no nutrients were analyzed in this work, periods with the highest ϕ_m are perceived to follow the nutrient injection to surface, facilitated by the breakdown of the thermocline and vertical recirculation in the water column (**Figures 5B,C**), which implies

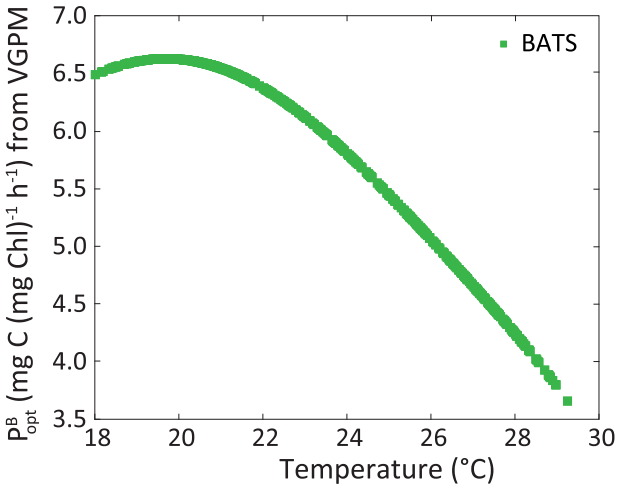

FIGURE 11 | Maximum C fixation rate within a water column [P^B_{opt}, in mg C (mg Chl)$^{-1}$ h^{-1}] following VGPM, as a function of SST_{sat} at BATS.

lower temperatures. There appears to be a reduction in metabolic rates under 20°C. However, during winter conditions, nutrient concentration was expected to be the highest, stimulating phytoplankton production and overriding any limitation caused by temperatures being under its optimum. This relation between ϕ_m, temperature, and nutrients explains the inverse relation between ϕ_m and SST_{sat}, supporting the idea of using this environmental parameter to model ϕ_m. The exploration of this relationship should be evaluated carefully at higher latitudes, where temperatures in winter can drop considerably thus the impact to ϕ_m separated from that by nutrient would be complex. Also, coastal environments can behave differently and SST_{sat} would not necessarily be a good proxy of the ϕ_m, since nutrient input also has a terrestrial contribution in addition to vertical stratification and the position of the thermocline.

It was shown here temporal variability of ϕ_m and K_ϕ estimated from *in situ* experiments of $PP_{in\ situ}$ and measurements of E_d and PAR at surface. Such estimation was only possible thanks to the effort of many people engaged to maintain long time-series measurements, with careful collection methods at HOT and BATS. These activities should be encouraged worldwide as we see that *in situ* observations are critical for calibration and validation activities into remote sensing science to allow it to provide reliable products. It appears that there is a better performance at HOT than at BATS, likely because we have a much bigger data pool at HOT than at BATS for the derivation of ϕ_m and K_ϕ. It thus allowed a better calibration of the model in the Pacific Ocean, improving $PP_{sat-aphy-based}$ performance. Also at BATS, the number of samples during some months (Jan, May, Nov, and Dec) was a bit lower than other months considering the coefficient of variation. Sorensen and Siegel (2001) showed a difference up to 40% along 4 consecutive days at BATS, exemplifying how highly noisy $PP_{in\ situ}$ can be. This suggests that, even with a great effort in keeping a long time-series of 26 years, *in situ* sampling could not be sufficient during some periods to

capture the real variability that could explain differences between $PP_{in\ situ}$ and $PP_{sat-aphy-based}$.

Within vegetal cells, only chlorophyll-a contributes to photosynthesis. Based on this premise, the $PP_{sat-chl-based}$ methods propose that PP can be directly estimated from Chl. However, there are some caveats in estimating PP with this strategy. First, even when Chl has been widely considered an indicator of phytoplankton biomass it is also known that Chl is a weak indicator of it (Behrenfeld et al., 2005, 2016; Bellacicco et al., 2016). It has been demonstrated that pigment concentration is dependent on the phytoplankton group, cell size, light availability, nutritional state of the cells, meaning that the same Chl value can be found in waters with different abundance of phytoplankton. Second, there are other accessory pigments in phytoplankton cells that also capture photons, which can be transmitted to chlorophyll-a and used in photosynthesis (if they are photosynthetic pigments, as for example, chlorophyll-b and -c) or this energy is lost as heat (when the implicated pigments are photoprotective, as for example diadinoxanthin and diatoxanthin) (Ostrowska et al., 2012). On the other hand, not all chlorophyll-a is active for photosynthesis. It is well known that it can exist as a "package" inside the cell, which means the capacity to absorb photons can be different even for the same Chl value. But these are not the only factors to take into account when evaluating the result of $PP_{sat-chl-based}$ models. Satellite sensors actually measures radiometric magnitude (i.e., radiance). The direct parameters we can derivate from those satellite measurements are, then, optical parameters (absorption, backscattering) rather than biological information such as Chl, which constitutes a secondary measurement. This suggests that $PP_{sat-aphy-based}$, that uses a phytoplankton absorption coefficient as input, reduces uncertainties in model inputs. In this context, ϕ is a key parameter that introduces biological information into the model that converts optical (absorbed light) into biological information (PP).

It is exactly to those optical and photophysiological parameters to whom researchers have attributed the responsibility for the low performance found in some PP_{sat} models that have been commonly applied (Platt et al., 1991; Morel et al., 1996; Bouman et al., 2000). Kovač et al. (2017) also point to the relation between the rate of carbon assimilation by phytoplankton and light as the core parameters that convert stocks of C (the immediate image taken by satellite) into a rate (PP). We demonstrated here that actually *questionable* photophysiological parameters are responsible for high uncertainties observed frequently in PP_{sat} results. In fact, the mathematical formulation of the $PP_{sat-aphy-based}$ and the optical inputs appear to be adequate. The part of the model that is still a challenge is in the linkage between optics and biology, that is, the quantum yield of photosynthesis. More efforts into the estimation of global ocean PP via satellite remote sensing should be allocated to *in situ* sampling to provide data to model this parameter. We showed that appropriate, spectrally resolved, inputs [$a_{phy}(\lambda)$ and $E_d(z, \lambda)$] combined with regionalized biological parameters reduce such uncertainties in producing reliable PP estimates over the years. This work shows also an example of how important regional studies are, and that the same biome in two different places, oligotrophic gyres in this case, can present different temporal behaviors in photosynthetic restrictions. We suggest that the formula to provide good estimates of oceanic primary production in the global ocean seems to be combining satellite observations with regionalized dynamical parameterization based on *in situ* measurements and using biogeochemical provinces as a frame for such regionalization.

CONCLUSIONS

Temporal and regional variability were observed in photophysiological parameters ϕ_m and K_ϕ estimated from decades of *in situ* measurements. At HOT, into the North Pacific Subtropical Gyre, the median annual values for ϕ_m and K_ϕ were 0.040 mol C mol photons^{-1} and 8.0 mol photons m^{-2} d^{-1}, respectively. Slightly higher values were found for both at BATS, located in the North Atlantic Subtropical Gyre, where ϕ_m was found equal to 0.063 mol C mol photons^{-1} and K_ϕ of 10.8 mol photons m^{-2} d^{-1}. In both regions, highest values of ϕ_m occurred in the Fall-Winter period, coinciding with the highest nutrient concentration. The peak of K_ϕ, on the contrary, was found in Summer, following seasonality in PAR. SST and $PAR_{day}(0^+)$ were chosen as proxies to estimate temporal variability of ϕ_m and K_ϕ, respectively. However, at HOT, seasonal variability seems negligible for ϕ_m and we kept it as a constant in this region equal to the annual median value derived from *in situ* measurements. Our dynamic parameterization was tested using satellite information and further applied to the $PP_{sat-aphy-based}$ model. The values found from such dynamic parameterization were within the same range as those from *in situ* measurements: 0.060 mol C mol photons^{-1} for ϕ_m at BATS, and 9.5 and 15.7 mol photons m^{-2} d^{-1} for K_ϕ, corresponding to HOT and BATS, respectively. Comparing with *in situ* measurements, the $PP_{sat-aphy-based}$ showed the same temporal variability, with differences of only 8.3% at HOT and 36.4% at BATS when our dynamic parameterization was used. These differences were lower than the ones found using a default $PP_{sat-chl-based}$ model at HOT which resulted in 62.8% difference, and similar at BATS, with AUPD of 37.8%. However, in terms of the seasonal pattern the $PP_{sat-chl-based}$ model performed worse in both areas ($R^2 = 0.27$ and 0.34 at HOT and BATS, respectively) and an opposite seasonal pattern at HOT. Our results strongly suggest that an effort to regionally parameterize ϕ_m and K_ϕ from *in situ* data can significantly improve PP_{sat}, to provide then, solid estimates of primary production of the global oceans.

AUTHOR CONTRIBUTIONS

MZ conceptualization, data processing and analysis, investigation, methodology, writing–original draft. ZL conceptualization, data analysis, investigation, methodology, writing–original draft, funding acquisition, project

administration, resources. JM conceptualization, data analysis, writing–original draft.

FUNDING

Funding for this study was provided by National Aeronautic and Space Administration (NNX14AM15G, NNX14AQ47A).

ACKNOWLEDGMENTS

The measurements and data collected at HOT and BATS are greatly appreciated. We thank NASA OBPG for providing products from ocean color satellite measurements, and two reviewers to improve this manuscript.

REFERENCES

Babin, M., Morel, A., Claustre, H., Bricaud, A., Kolbert, Z., and Falkowski, P. G. (1996). Nitrogen- and irradiancedependent variations of the maximum quantum yield of carbon fixation in eutrophic, mesotrophic and oligotrophic marine systems. *Deep-Sea Res. Part I*. 43, 1241–1272. doi: 10.1016/0967-0637(96)00058-1

Bates, N. R., Michaels, A. F., and Knap, A. H. (1996). Seasonal and interannual variability of oceanic carbon dioxide species at the U.S. JGOFS bermuda atlantic time-series study (BATS) site. Deep-Sea Res. *Part II*. 43, 347–383. doi: 10.1016/0967-0645(95)00093-3

Behrenfeld, M. J., Boss, E. S., Siegel, D. A., and Shea, D. M. (2005). Carbon-based ocean productivity and phytoplankton physiology from space. *Global Biogeochem. Cycles* 19:GB1006. doi: 10.1029/2004GB002299

Behrenfeld, M. J., and Falkowski, P. G. (1997a). A consume's guide to phytoplankton primary productivity models. *Limnol. Oceanogr*. 42, 1479–1491.

Behrenfeld, M. J., and Falkowski, P. G. (1997b). Photosynthetic rates derived from satellite-based chlorophyll concentration. *Limnol. Oceanogr*. 42, 1–20. doi: 10.4319/lo.1997.42.1.0001

Behrenfeld, M. J., O'Malley, R. T., Boss, E. S., Westberry, T. K., Graff, J. R., Halsey, K. H., et al. (2016). Revaluating ocean warming impacts on global phytoplankton. *Nat. Clim. Chang*. 6, 323–330. doi: 10.1038/nclimate2838

Behrenfeld, M. J., Randerson, J. T., McClain, C. R., Feldman, G. C., Los, S. O., Tucker, C. J., et al. (2001). Biospheric primary production during an ENSO transition, *Science* 291, 2594–2597. doi: 10.1126/science.1055071

Bellacicco, M., Volpe, G., Colella, S., Pitarch, J., and Santoleri, R. (2016). Influence of photoacclimation on the phytoplankton seasonal cycle in the mediterranean sea as seen by satellite. *Remote Sens. Environ*. 184, 595–604. doi: 10.1016/j.rse.2016.08.004

Bidigare, R., Michael, E. O., Morrow, J. H., and Kiefer, D. A. (1990). *In vivo* absorption properties of algal pigments. *Proc. SPIE–Int. Soc. Opt. Eng*. 1302, 290–302.

Bouman, H. A., Platt, T., Sathyendranath, S., Irwin, B. D., Wernand, M. R., and Kraay, G. W. (2000). Bio-optical properties of the Subtropical North Atlantic. II. relevance to models of primary production. *Mar. Ecol. Prog. Ser*. 200, 19–34. doi: 10.3354/meps200019

Campbell, J., Antoine, D., Armstrong, R., Arrigo, K., Balch, W., Barber, R., et al. (2002). Comparison of algorithms for estimating ocean primary production from surface chlorophyll, temperature, and irradiance. *Global Biogeochem. Cy*. 16:1035. doi: 10.1029/2001GB001444.

Carder, K. L., Lee, Z., Marra, J., Steward, R. G., and Perry, M. J. (1995). Calculated quantum yield of photosynthesis of phytoplankton in the marine light-mixed layers (59-Degrees-N, 21-Degrees-W). *J. Geophys. Res. Oceans* 100, 6655–6663. doi: 10.1029/94JC02793

Carr, M. E., Friedrichs, M. A. M., Schmeltz, M., Noguchi Aita, M., Antoine, D., Arrigo, K. R., et al. (2006). A comparison of global estimates of marine primary production from ocean color. *Deep-Sea Res. II*. 53, 741–777. doi: 10.1016/j.dsr2.2006.01.028

Falkowski, P. G. (1980). "Light-shade adaptation in marine phytoplankton", in *Primary Productivity in the Sea*, ed P. Falkowski (New York, NY: Plenum Press), 99–119.

Field, C. B., Behrenfeld, M. J., Randerson, J. T., and Falwoski, P. G. (1998). Primary production of the biosphere: integrating terrestrial and oceanic components. *Science* 281, 237–240. doi: 10.1126/science.281.5374.237

Finenko, Z. Z., Churilova, T. Y., Sosik, H. M., and Basturk, O. (2002). Variability of photosynthetic parameters of the surface phytoplankton in the Black Sea. *Okeanologiya* 42, 53–67.

Fitzwater, S. E., Knauer, G. A., and Martin, J. H. (1982). Metal contamination and its effects on primary production measurements. *Limnol. Oceanogr*. 27, 544–551. doi: 10.4319/lo.1982.27.3.0544

Frouin, R., Lingner, D. W., Gautier, C., Baker, K. S., and Smith, R. C. (1989). A simple analytical formula to compute clear sky total and photosynthetically available solar irradiance at the ocean surface. *J. Geophys. Res*. 94, 9731–9742. doi: 10.1029/JC094iC07p09731

Hirawake, T., Takao, S., Horimoto, N., Ishimaru, T., Yamaguchi, Y., and Fukuchi, M. (2011). A phytoplankton absorption-based primary productivity model for remote sensing in the Southern Ocean. *Polar Biol*. 34, 291–302. doi: 10.1007/s00300-010-0949-y

Iluz, D., and Dubinsky, Z. (2013). "Quantum yields in aquatic photosynthesis", in *Photosynthesis*, ed Z. Dubinsky (IntechOpen), 135–158. doi: 10.5772/56539

Karl, D. M., Christian, J. R., Dore, J. E., Hebel, D. V., Letelier, R. M., Tupas, L. M., et al. (1996). Seasonal and interannual variability in primary production and particle flux at station ALOHA. *Deep-Sea Res. Part II*. 43, 539–568. doi: 10.1016/0967-0645(96)00002-1

Karl, D. M., and Church, M. J. (2017). Ecosystem structure and dynamics in the north pacific subtropical gyre: new views of an old ocean. *Ecosystems* 20, 433–457. doi: 10.1007/s10021-017-0117-0

Kiefer, D., and Mitchell, B. G. (1983). A simple, steady state description of phytoplankton growth based on absorption cross section and quantum efficiency. *Limnol. Oceanogr*. 28, 770–776. doi: 10.4319/lo.1983.28.4.0770

Kishino, M., Takahashi, M., Okami, N., and Ichimura, S. (1985). Estimation of the spectral absorption coefficients of phytoplankton in the sea. *Bull. Mar. Sci*. 37, 634–642.

Kolber, Z. S., Prasil, O., and Falkowski, P. G. (1998). Measurements of variable chlorophyll fluorescence using fast repetition rate techniques: defining methodology and experimental protocols. *Biochim. Biophys. Acta* 1367, 88–106. doi: 10.1016/S0005-2728(98)00135-2

Kovač, Ž., Platt, T., Sathyendranath, S., and Antunović, S. (2017). Models for estimating photosynthesis parameters from *in situ* production profiles. *Prog. Oceanogr*. 159, 255–266. doi: 10.1016/j.pocean.2017.10.013

Lee, Z. (2014). *Update of the Quasi-Analytical Algorithm (QAA_v6)*. Dartmouth: International Ocean Colour Coordinating Group. Available online at: http://www.ioccg.org/groups/Software_OCA/QAA_v6_2014209.pdf

Lee, Z., Carder, K. L., and Arnone, R. A. (2002). Deriving inherent optical properties from water color: a multiband quasi-analytical algorithm for optically deep waters. *Appl. Opt*. 41, 5755–5772. doi: 10.1364/AO.41.005755

Lee, Z., Carder, K. L., Mobley, C. D., Steward, R. G., and Patch, J. S. (1999). Hyperspectral remote sensing for shallow waters. 2. deriving bottom depths and water properties by optimization. *Appl. Opt*. 38, 3831–3843.

Lee, Z., Du, K., and Arnone, R. (2005a). A model for the diffuse attenuation coefficient of downwelling irradiance. *J. Geophys. Res. Oceans*. 110, 1–10. doi: 10.1029/2004JC002275

Lee, Z., Du, K., Arnone, R., Liew, S. C., and Penta, B. (2005b). Penetration of solar radiation in the upper ocean – a numerical model for oceanic and coastal waters. *J. Geophys. Res*. 110:C09019. doi: 10.1029/2004JC002780

Lee, Z., Hu, C., Shang, S., Du, K., Lewis, M., Arnone, R., et al. (2013). Penetration of UV-visible solar radiation in the global oceans: insights from ocean color remote sensing. *J. Geophys. Res. Oceans*. 118, 4241–4255. doi: 10.1002/jgrc.20308

Lee, Z., Lance, V. P., Shang, S., Vaillancourt, R., Freeman, S., Lubac, B., et al. (2011). An assessment of optical properties and primary production derived from remote sensing in the southern ocean (SO GasEx). *J. Geophys. Res*. 116, 1–15. doi: 10.1029/2010JC006747

Lee, Z., Marra, J., Perry, M. J., and Kahru, M. (2015). Estimating oceanic primary productivity from ocean color remote sensing: a strategic assessment. *J. Mar. Syst*. 149, 50–59. doi: 10.1016/j.jmarsys.2014.11.015

Lee, Z. P., Carder, K. L., Marra, J., Steward, R. G., and Perry, M. J. (1996). Estimating primary production at depth from remote sensing. *Appl. Opt*. 35, 463–474. doi: 10.1364/AO.35.000463

Letelier, R. M., Bidigare, R. R., Hebel, D. V., Ondrusek, M., Winn, C. D., and Karl, D. M. (1993). Temporal variability of phytoplankton community structure based on pigment analysis. *Limnol. Oceanogr*. 38, 1420–1437. doi: 10.4319/lo.1993.38.7.1420

Li, W. K. W. (1980). "Temperature adaptation in phytoplankton: cellular and photosynthetic characteristics", in *Primary Productivity in the Sea*, ed P. Falkowski (New York, NY: Plenum Press), 259–279.

Longhurst, A., Sathyendranath, S., Platt, T., and Caverhill, C. (1995). An estimate of global primary production in the ocean from satellite radiometer data. *J. Plankton Res*. 17, 1245–1271. doi: 10.1093/plankt/17.6.1245

Ma, S., Tao, Z., Yang, X., Ma, W., Yu, Y., Zhou, X., et al. (2014). Estimation of marine primary productivity from satellite-derived phytoplankton absorption data. *J-STARS* 7, 3084–3092. doi: 10.1109/JSTARS.2014.2298863

Marra, J., Chamberlain, W. S., and Knudson, C. (1993). Proportionality between *in situ* carbon assimilation bio-optical measures of primary production in the gulf of maine in summer. *Limnol. Oceanogr*. 38, 232–238. doi: 10.4319/lo.1993.38.1.0232

Marra, J., Trees, C. C., Bidigare, R. R., and Barber, R. T. (2000). Pigment absorption and quantum yields in the Arabian Sea. *Deep-Sea Res. Part I*. 47, 1279–1299. doi: 10.1016/S0967-0645(99)00144-7

Menzel, D. W., and Ryther, J. H. (1960). The annual cycle of primary production in the Sargasso Sea off Bermuda. *Deep-Sea Res.* 6, 351–367.

Mobley, C. D., and Sundman, L. K. (2008). *HydroLight Technical Documentation*. Bellevue, WA: Sequoia Scientific, Inc.

Morel, A. (1978). Available, usable, and stored radiant energy in relation to marine photosynthesis. *Deep-Sea Res*. 25, 673–688. doi: 10.1016/0146-6291(78)90623-9

Morel, A., Antoine, D., Babin, M., and Dandonneau, Y. (1996). Measured and modeled primary production in the Northeast Atlantic (EUMELI JGOFS Program): the impact of natural variations in photosynthetic parameters on model predictive skill. *Deep-Sea Res*. 43, 1273–1304. doi: 10.1016/0967-0637(96)00059-3

Morrison, J. R., and Nelson, N. B. (2004). Seasonal cycle of phytoplankton UV absorption at the Bermuda Atlantic Time-Series Study (BATS) Site. *Limnol. Oceanogr*. 49, 215–224. doi: 10.4319/lo.2004.49.1.0215

NASA (2003). *Ocean Optics Protocols for Satellite Ocean Color Sensor Validation (Rev. 4, Vol. III: Radiometric Measurements and Data Analysis Protocols NASA/NASA/TM-2003–21621/Rev-Vol III)*. NASA, Goddard Space Flight Space Center, Greenbelt, MD.

Ostrowska, M., Wozniak, B., and Dera, J. (2012). Modelled quantum yields and energy efficiency of fluorescence, photosynthesis and heat production by phytoplankton in the World Ocean. *Oceanologia* 54, 565–610. doi: 10.5697/oc.54-4.565

Platt, T., Caverhill, C., and Sathyendranath, S. (1991). Basin-Scale estimates of oceanic primary production by remote sensing: the North Atlantic. *J. Geophys. Res*. 96, 15147–15159. doi: 10.1029/91JC01118

Platt, T., and Sathyendranath, S. (1988). Oceanic primary production: estimation by remote sensing at local and regional scales. *Science* 241, 1613–1619. doi: 10.1126/science.241.4873.1613

Platt, T., Shubba-Rao, D. V., and Irwin, B. (1983). Photosynthesis of Picoplankton in the Oligotrophic Ocean. *Nature* 301, 702–704.

Ratkowsky, D. A., Lowry, R. K., McMeekin, T. A., Stokes, A. N., and Chandler, R. E. (1983). Model for bacterial culture growth rate throughout the entire biokinetic temperature range. *J. Bacteriol*. 154, 1222–1226.

Saba, V. S., Friedrichs, M. A. M., Carr, M. E., Antoine, D., Armstrong, R. A., Asanuma, I., et al. (2010). Challenges of modeling depth-integrated marine primary productivity over multiple decades: a case study at BATS and HOT. *Global Biogeochem. Cy*. 24, 1–21. doi: 10.1029/2009GB003655

Siegel, D. A., Iturriaga, R., Bidigare, R. R., Pak, H., Smith, R. C., Dickey, T. D., et al. (1990). Meridional variations of the springtime Phytoplankton community in the Sargasso Sea. *J. Mar. Res*. 48, 379–412. doi: 10.1357/002224090784988791

Sorensen, J. C., and Siegel, D. A. (2001). Variability of the effective quantum yield for carbon assimilation in the Sargasso Sea. *Deep-Sea Res. Part II Top. Stud. Oceanogr*. 48, 2005–2035. doi: 10.1016/S0967-0645(00)00170-3

Steinberg, D. K., Carlson, C. A., Bates, N. R., Johnson, R. J., Michaels, A. F., and Knap, A. H. (2001). Overview of the US JGOFS Bermuda Atlantic Time-Series Study (BATS): a decade-scale look at ocean biology and biogeochemistry. *Deep-Sea Res. Part II Top. Stud. Oceanogr*. 48, 1405–1447. doi: 10.1016/S0967-0645(00)00148-X

Werdell, P. J., Franz, B. A., Bailey, S. W., Feldman, G. C., Boss, E., Brando, V. E., et al. (2013). Generalized ocean color inversion model for retrieving marine inherent optical properties. *Appl. Opt*. 52:2019. doi: 10.1364/AO.52.002019

Westberry, T., Behrenfeld, M. J., Siegel, D. A., and Boss, E. Carbon-based primary productivity modeling with vertically resolved photoacclimation. (2008). *Global Biogeochem. Cy*. 22:GB2024. doi: 10.1029/2007GB003078

Wozniak, B., Dera, J., Ficek, D., Majchrowski, R., Kaczmarek, S., Ostrowska, M., et al. (1999). Modelling the influence of acclimation on the absorption properties of marine phytoplankton. *Oceanologia* 41, 187–210.

Zoffoli, M. L., Lee, Z., Ondrusek, M., Lin, J., Kovach, C., Wei, J., et al. (2017). Estimation of transmittance of solar radiation in the visible domain based on remote sensing: evaluation of models using *in situ* data. *J. Geophys. Res. Oceans* 122, 1–13. doi: 10.1002/2017JC013209

Conflict of Interest Statement: The authors declare that the research was conducted in the absence of any commercial or financial relationships that could be construed as a potential conflict of interest.

APPENDIX

TABLE A1 | Normalized spectra [$\bar{E}_S(\lambda)$, dimensionless] for the visible spectra (400–700 nm).

λ (nm)	$\bar{E}_S$	λ (nm)	$\bar{E}_S$	λ (nm)	$\bar{E}_S$	λ (nm)	$\bar{E}_S$	λ (nm)	$\bar{E}_S$
400	0.00252	460	0.00372	520	0.00349	580	0.00353	640	0.00323
402	0.00279	462	0.00371	522	0.00359	582	0.00355	642	0.00322
404	0.00283	464	0.00371	524	0.00360	584	0.00349	644	0.00317
406	0.00279	466	0.00370	526	0.00358	586	0.00339	646	0.00312
408	0.00279	468	0.00371	528	0.00356	588	0.00331	648	0.00307
410	0.00288	470	0.00372	530	0.00358	590	0.00328	650	0.00307
412	0.00296	472	0.00373	532	0.00359	592	0.00326	652	0.00307
414	0.00299	474	0.00376	534	0.00361	594	0.00328	654	0.00303
416	0.00301	476	0.00379	536	0.00362	596	0.00331	656	0.00297
418	0.00302	478	0.00381	538	0.00362	598	0.00334	658	0.00295
420	0.00301	480	0.00380	540	0.00359	600	0.00336	660	0.00303
422	0.00300	482	0.00379	542	0.00357	602	0.00338	662	0.00311
424	0.00293	484	0.00370	544	0.00357	604	0.00339	664	0.00313
426	0.00284	486	0.00360	546	0.00358	606	0.00340	666	0.00312
428	0.00276	488	0.00354	548	0.00359	608	0.00340	668	0.00311
430	0.00275	490	0.00363	550	0.00359	610	0.00336	670	0.00310
432	0.00274	492	0.00372	552	0.00359	612	0.00333	672	0.00308
434	0.00287	494	0.00373	554	0.00357	614	0.00332	674	0.00307
436	0.00305	496	0.00371	556	0.00353	616	0.00331	676	0.00306
438	0.00321	498	0.00369	558	0.00351	618	0.00331	678	0.00305
440	0.00330	500	0.00363	560	0.00353	620	0.00331	680	0.00304
442	0.00339	502	0.00358	562	0.00355	622	0.00331	682	0.00302
444	0.00346	504	0.00361	564	0.00353	624	0.00329	684	0.00290
446	0.00353	506	0.00367	566	0.00351	626	0.00326	686	0.00275
448	0.00359	508	0.00371	568	0.00349	628	0.00323	688	0.00264
450	0.00365	510	0.00368	570	0.00350	630	0.00323	690	0.00265
452	0.00370	512	0.00364	572	0.00351	632	0.00323	692	0.00266
454	0.00372	514	0.00356	574	0.00351	634	0.00324	694	0.00269
456	0.00373	516	0.00345	576	0.00351	636	0.00324	696	0.00272
458	0.00373	518	0.00340	578	0.00351	638	0.00325	698	0.00274
								700	0.00272